Entropy in the molecular recognition of membrane protein-lipid interactions

Pei Qiao[1], Samantha Schrecke[2], Thomas Walker[2], Jacob W. McCabe[2], Jixing Lyu[2], Yun Zhu[2], Tianqi Zhang[2], Smriti Kumar[2], David Clemmer[3], David H. Russell[2], Arthur Laganowsky[2,*]

[1]Department of Biochemistry and Biophysics, Texas A&M University, College Station, TX 77843
[2]Department of Chemistry, Texas A&M University, College Station, TX 77843
[3]Department of Chemistry, Indiana University, Bloomington, IN 47405

*Corresponding Author: ALaganowsky@chem.tamu.edu

Abstract
Understanding the molecular driving forces that underlie membrane protein-lipid interactions requires the characterization of their binding thermodynamics. Here, we employ native mass spectrometry in conjunction with a variable temperature apparatus to determine the thermodynamics of individual lipid binding events to the human G-protein-gated inward rectifier potassium channel, Kir3.2. We find that Kir3.2 displays distinct thermodynamic strategies to engage phosphatidylinositol (PI) and phosphorylated forms thereof. The addition of a 4'-phosphate to PI with 18:1-18:1 (DO) tails results in an increase in favorable entropy along with an enthalpic penalty. The binding of PI with two or more phosphates is more complex where lipids bind to Kir3.2 with the cytoplasmic domain in either a docked or extended configuration. Remarkably, the interaction of 4,5-bisphosphate DOPI (DOPI(4,5)P_2) with Kir3.2 is solely driven by a large, favorable change in entropy. Installment of a third 3'-phosphate to DOPI(4,5)P_2 results in an alternative thermodynamic strategy for the first binding event whereas each successive binding event shows strong enthalpy-entropy compensation. PI(4,5)P_2 with 18:0-20:4 tails results in an inversion of thermodynamic parameters where the change in enthalpy now dominates. Collectively, the data show that entropy can indeed play important roles in regulating membrane protein-lipid interactions.

Introduction
Inward rectifier potassium (Kir) channels are expressed in tissues throughout the body where they play central roles in many physiological processes, such as parasympathetic slowing of the heart[1], pain perception[2], and pancreatic insulin secretion.[3-9] Some mutations in these channels result in improper trafficking that is associated with Andersen syndrome.[10] In particular, phosphatidylinositol 4,5-bisphosphate (PI(4,5)P_2), a minor component of the cytoplasmic leaflet,[11] is required for activation of all Kir channels.[12-15] Kir channels are also regulated by many other molecules including phosphorylation by kinases, sodium, pore blockers (polyamine, Mg^{2+}), and ethanol.[10, 16, 17] There are seven subfamilies of Kir channels: classical Kir channels (Kir2.x) are strong rectifiers that have central roles in cardiac inward rectifier current; Kir3.x channels are unique in that they require $G_{\beta\gamma}$ in addition to PIP_2 for function with some of these channels modulated by sodium ions; ATP-sensitive potassium channels (Kir6.x); and transport potassium channels (Kir1.x, Kir4.x, Kir5.x, and Kir7.x).[9, 10, 18-21]

All Kir channels form tetrameric complexes composed of similar or different subunits.[15, 22, 23] Each subunit encodes two transmembrane domains (TMD), in which the K^+ selectivity filter resides, that is tethered by a short linker to the cytoplasmic domain (CTD).[22, 23] Structures have also revealed a PI(4,5)P_2 binding pocket located at the interface of the TMD and CTD.[15, 23] The binding pocket is a highly conserved region consisting of a set positively charged amino acid residues that engage the phosphorylated headgroup of PI(4,5)P_2.[15, 23, 24] Mutations in residues important for binding the signaling lipid are associated with Bartter and Andersen syndromes, and other diseases.[5, 25, 26] The specific lipid binding site within Kir channels has garnered the attention of computational studies to identify and predict lipid-binding sites on ion channels.[27-30]

Kir channels have varied specificity and varying degrees of channel activation by the different phosphoinositides. All Kir channels are maximally activated by PI(4,5)P_2 and, in some cases, PI(4,5)P_2 is the only phosphoinositide (PIP) that stimulates activity.[13, 31, 32] In contrast, Kir6.x appears to be promiscuously activated by PI(3,4)P_2, PI(4,5)P_2 and PI(3,4,5)P_3.[31, 32] The acyl chain composition has also been shown to be a contributing factor to the level of stimulation, such as Kir3.1/Kir3.4 channels display preference for PI(4,5)P_2 with 18:0-20:4 (SA) acyl chain whereas Kir2.1 shows no preference towards acyl chains.[33] The concentration dependence of PI(4,5)P_2 activation of Kir3.2 in a lipid bilayer exhibits positive cooperativity.[34] Similar observations were made by employing a soluble fluorescent lipid binding assay wherein the binding of a fluorophore modified PI(4,5)P_2 to Kir3.2 fused to a fluorescent protein is monitored by Förster resonance energy transfer.[35]

Historically it has been difficult to dissect and interrogate lipid binding events to membrane proteins, which is necessary to fully characterize binding thermodynamics. Recently, native mass spectrometry (MS) has emerged as an indispensable biophysical technique for characterizing membrane proteins and their interactions with lipids and other molecules, such as regulatory proteins.[36] In contrast to other biophysical techniques that report on the ensemble, native MS can not only capture a snapshot of solution equilibria but also resolve individual ligand-bound states of membrane protein complexes.[37] Over the past decade, native MS has discovered the role of specific lipids in stabilizing membrane protein complexes,[37-39] allosteric modulation of membrane protein interactions with protein,[40, 41] lipids,[42] and drugs,[43-46] and those important for function,[37, 44-48] such as PI(4,5)P_2 in G-protein-coupled receptor activation and G-protein selectivity.[41] Lipid and toxin binding to Kir3.2 has been interrogated using native MS that has provided insight into the binding preferences for PIPs.[49] Native MS combined with mutational studies has shed light on the contribution of amino acids in the PIP binding site of Kir3.2 and how they impact binding preferences for PIPs.[35] Despite progress in understanding Kir-lipid interactions, the thermodynamics for the association of lipids with Kir3.2 have been enigmatic.

Results

To determine the thermodynamic basis for Kir3.2-lipid interactions, we used native MS coupled with a variable-temperature nanoelectrospray ionization (nESI) apparatus to determine through van't Hoff analysis the change in enthalpy (ΔH) and entropy ($-T\Delta S$), components of the change in Gibbs free energy (ΔG).[50, 51] The first set of lipids we investigated were dioleoyl (18:1-18:1) phosphatidylinositol (DOPI) and phosphatidylinositol 4-phosphate with DO tails (DOPI(4)P). Here,

we focus our initial discussion on DOPI(4)P as up to three bound Kir3.2 whereas only one DOPI bound the channel (**Figure S1 and S2**). More specifically, Kir3.2 solubilized in $C_{10}E_5$, a detergent that in the nESI process results in charge reduced ions that aids preservation of non-covalent interactions and native-like structure in the mass spectrometer,[37, 52] at a concentration of 0.25 µM was titrated with DOPI(4)P up to a final concentration of 2.5 µM. These samples were then incubated online using a variable temperature nESI apparatus[53] for several minutes to reach equilibrium followed by acquiring their native mass spectra (**Figure 1A, S3 and S4**). The mass spectra from this titration series at a given temperature were deconvoluted using UniDec[54] and the abundance of Kir3.2•DOPI(4)P_{0-3} was used to compute the mole fraction for the different lipid-bound states (**Figure 1B**). A sequential ligand binding model was fit to the mole fraction data to determine the equilibrium binding constants at a given temperature (**Figure 1B**). Thermodynamics for the individual DOPI(4)P binding events to Kir3.2 was deduced through van't Hoff analysis[50] (**Figure 1C**). Interestingly, the binding of one to three DOPI(4)P molecules to Kir3.2 is driven by entropy and the enthalpic term near zero (**Figure 1D**). This result is in complete contrast to our previous study of the bacterial ammonia channel (AmtB) binding phospholipids where the binding was driven by enthalpy and, in most cases, entropy was unfavorable.[51] The thermodynamic parameters for each DOPI(4)P binding event are statistically indistinguishable. Thermodynamics for the binding of one DOPI to Kir3.2 was determined in a similar fashion as done for DOPI(4)P. The binding of this lipid is also largely driven by entropy with a marginal favorable contribution from entropy (**Figure S11 and S14**).

To better understand the molecular forces that underlie their molecular recognition, we next focused on other phosphorylated forms of phosphatidylinositol known to activate Kir3.2 and other channels. These lipids include 4,5-bisphosphate PI with DO (DOPI(4,5)P_2) and 1-stearoyl-2-arachidonoyl (SAPI(4,5)P_2) tails and 3,4,5-trisphosphate PI with DO (DOPI(3,4,5)P_3). In a similar fashion as described above, we first titrated Kir3.2 with DOPI(4,5)P_2 and recorded their native mass spectra at different temperatures (**Figure S5 and S6**). Regardless of the temperature, the application of a sequential lipid binding model resulted in poor fits, especially for the first and second lipid bound states of Kir3.2 (**Figure S12**). Specifically, the trend in the mole fraction data for the first and second binding event does not follow a smooth curve but is asymptotic at higher lipid concentrations suggestive of two underlying binding distributions. Although first described for Kir2.2 (**Figure 2A**),[15] recent structures of Kir3.2 have shown it also populates two distinct conformations where the CTD is docked, forming contacts with the cytoplasmic face of the TMD, or in an extended state, CTD displaced from the transmembrane domain.[55, 56] Modification of the lipid binding model such that the first and second lipid binding events bind to either a docked or extended states (**see Methods**) resulted in substantially improved fits (**Figure 2B and S12**). Here, the binding of the third lipid to Kir3.2 could represent a transition point wherein the three bounds lipid drive the channel from an extended to the docked state. This is consistent with recent cryoEM studies showing a population shift in the abundance of the docked state with increasing concentrations of PI(4,5)P_2.[55, 56]

Application of lipid binding model to different states of Kir3.2 was used to determine the K_D for each lipid binding event at a given temperature followed by van't Hoff analysis(**Figure 2C and S14**). The K_Ds for one to four DOPI(4,5)P_2 binding events to the docked state of Kir3.2 display

positive cooperativity (**Table S1**). Surprisingly, the thermodynamics for DOPI(4,5)P_2 associating with Kir3.2 reveal that the molecular driving force is solely entropic, outweighing an enthalpic penalty, regardless of binding to either the docked or extended state (**Figure 2C**). In the case of binding to the docked state, which we presume has a higher affinity for the lipid based on structures,[23, 24] unfavorable enthalpy was largest for the first binding event and subsequent binding events the thermodynamic parameters were similar. In contrast, the enthalpy for the binding event to the extended state increased. The additional 3'-phosphate on DOPI(3,4,5)P_3 resulted in distinct thermodynamic signatures in comparison to DOPI(4,5)P_2. Excluding the first binding event to the docked structure where it is driven by entropy and enthalpically unfavorable, all the other binding events showed enthalpy-entropy compensation whereby entropy and enthalpy were altered in opposing directions for each subsequent binding event (**Figure 2C**). Altering acyl chain chemistry of PI(4,5)P_2 to contain SA tails, resulting in a new subset of thermodynamic values with the majority of binding events driven by enthalpy. For binding to the docked state, favorable enthalpy was greatest for binding the first lipid whereas for second and third were similar but to a larger extent compared to the fourth. The fourth SAPI(4,5)P_2 binding event is unique among the PIPs investigated in that both entropy and enthalpy are favorable. Remarkably, these results demonstrate that specific phosphorylated forms of PI selectively engage the different states of Kir3.2.

It is striking when comparing the stepwise progression from DOPI to DOPI(3,4,5)P_3 and different acyl chains on binding thermodynamics (**Figure 3**). The addition of a 4-phosphate to DOPI pushes the reaction to be driven by entropy. Going from DOPI(4)P to DOPI(4,5)P_2 results in ~60 kJ/mol contributing to both enthalpy and entropy but in opposing directions for the first lipid binding. This is consistent for the other binding events but to half the extent. DOPI(3,4,5)P_3 with three phosphates displays a strong enthalpy-entropy dependence. A remarkable 175 kJ/mol alteration in thermodynamic parameters but in the opposing direction is observed for the first binding event of DOPI(3,4,5)P_3 to the docked state. Compared to DOPI(4,5)P_2, the binding of two or more DOPI(3,4,5)P_3 to Kir3.2 are accompanied by compensatory gains in favorable entropy and unfavorable enthalpy spanning 50 kJ/mol. The replacement of DOPI(4,5)P_2 with SA tails displayed marked gains in favorable enthalpy and unfavorable entropy, and the first SAPI(4,5)P_2 binding event had a remarkable change of nearly 200 kJ/mol. These results illustrate the marked impact on binding thermodynamics that can be observed with changing the chemistry of the lipid.

The thermodynamics of Kir3.2-lipid interactions provide rich chemical insight into the molecular forces underlying specific Kir3.2-lipid interactions. The majority of phosphorylated forms of DOPI binding events are driven by entropy and, in most cases, there is an unfavorable change in enthalpy. It is important to note these lipids possess DO tails and therefore the entropic contribution from desolvation of the acyl chains plays a minor role in the large entropies observed here. While solvent reorganization of the phosphorylated headgroup and/or PIP binding pocket of Kir3.2 can contribute in a positive way to entropy,[57, 58] the largely favorable entropy accompanied by unfavorable enthalpy observed here is reminiscent of soluble protein-ligand interactions that are driven by large conformational entropy originating in enhanced protein motions.[59-62] The first binding events of DOPI(4,5)P_2, DOPI(3,4,5)P_3, and SAPI(4,5)P_2 indicate significant structural changes upon binding. The thermodynamics for DOPI(4,5)P_2

suggests a significant enhancement in protein dynamics whereas for the two other lipids there is significant structuring of Kir3.2. We have previously observed enthalpy-entropy compensation for AmtB-lipid interactions.[51] However, the enthalpy-entropy compensation is more pronounced for Kir3.2-DOPI(3,4,5)P_3 in comparison to that observed for AmtB-lipid interactions and likely due to significant structuring of the channel at the cost of a reduction in disorder. The enthalpically driven binding of SAPI(4,5)P_2 to Kir3.2 suggests the SA tails interact more favorably with Kir3.2 in comparison to the lipid with DO tails.

Conclusions

In summary, the thermodynamics of lipids associating with Kir3.2 reveal different thermodynamic strategies. The changes observed for binding thermodynamics upon phosphorylation(s) of the inositol headgroup or altering the acyl chains are remarkable. Moreover, the association of Kir3.2 with specific PIPs can be driven by a large change in favorable entropy. This entropy is likely the result of considerable solvent reorganization as well as enhanced protein dynamics, which has been shown to underlie soluble protein-ligand interactions.[59, 61] High conformational entropy has recently been observed for two monomeric membrane proteins, independent of the membrane mimetic.[63] Here, we provide evidence that entropy can indeed greatly influence membrane protein-lipid interactions.

Materials and Methods

Plasmid construction and protein expression. The human Kir3.2 cDNA (KCNJ6, Uniprot P48051) was purchased from Horizon with a catalog number of MHS6278-202857476. Kir3.2 (residues 49-378), was cloned into a modified pACEBac1 insect cell expression vector (Geneva Biotech) with a C-terminal StrepTag II affinity tag by following the manufacturer's protocol. The expression plasmid has been deposited at Addgene plasmid #177263. The expression vector was transformed into *Ecoli* EmBacY (Geneva Biotech) cells and integrates of the expression cassette into the baculoviral genome were identified using blue/white colony screening following the manufacturer's protocol. A single white colony was inoculated overnight and recombinant baculoviral DNA was purified using HiPure Plasmid Midiprep kit (Invitrogen). The purified baculoviral genome DNA (30 µg) was mixed with 2ml PBS (NaCl 137 mM, KCl 2.7 mM, Na_2HPO_4 10 mM, KH_2PO_4 1.8 mM, pH 7.4) and PEI Max (Polysciences) transfection reagent (60 µl, 1 mg/ml in PBS).[64] After 20-min incubation, the mixture was added to *Spodoptera frugiperda* (Sf9) cells (30 ml, 0.8 x 10^6 cell/ml) in suspension and grown at 27 ^oC for a week to produce baculovirus. The clarified P1 was used to infect *Trichoplusia ni* (Tni) cells for protein expression and incubated at 27 ^oC for 2-3 days before harvesting. All insect cell lines and media are from Expression Systems LLC.

Protein purification. The post-infected Tni cells were harvested by centrifugation (4,000 g, 10 min, 4 ^oC). The cell pellets were resuspended in lysis buffer (300 mM KCl and 50 mM Tris pH7.4 at RT). The resuspended cell pellets were passed through a microfluidizer (M-110PS, Microfluidics Inc.) operating at 25,000 psi. The cell lysate was then clarified by centrifugation (25,000 g, 20 min, 4 ^oC) and the supernatant was subjected to ultracentrifugation (100,000g, 2hr, 4 ^oC) to harvest membranes. The membrane was resuspended in lysis buffer and homogenized using a glass

tissue blender (Wheaton). DDM (n-Dodecyl-β-D-Maltopyranoside, Glycon Biochemicals) was added to a final concentration of 2% to extract membrane proteins at 4 °C for 2 hours. The membrane protein extract was clarified by centrifugation (25,000 g, 20 min, 4 °C) before loading onto a drip column packed with streptactin Sepharose (IBA Biosciences) equilibrated with SPKHA buffer (150 mM KCl, 50 mM Tris, 10% glycerol, 0.025% DDM, pH 7.4 at RT). After loading the sample on the StrepTrap, 10 column volumes (CV) of SPKHA were used to wash the column, followed by a 10 CV wash of SPKHB (SPKHA with 0.025% DDM replaced by 6 mM DHPC [1,2-dihepanoyl-sn-glycero-3-phosphocholine]) and 10 CV wash of SPKHC (SPKHA with 0.025% DDM replaced by 0.065% $C_{10}E_5$ [Pentaethylene Glycol Monodecyl Ether]). The protein was then eluted with SPKHD buffer (SPKHC with 3mM D-desthiobiotin). The eluted sample was buffer exchanged into SPKHC using a desalting column. Protein concentration was measured using a DC protein assay (Bio-Rad). The purified protein was used immediately or stored at -80 °C.

Preparation and titration of phospholipids. 1,2-dioleoyl-phosphatidylinositol (DOPI), 1,2-dioleoyl-phosphatidylinositol-4'-phosphate (DOPI(4)P), 1,2-dioleoyl-phosphatidylinositol-4',5'-bisphosphate (DOPI(4,5)P_2), 1,2-dioleoyl-sn-glycero-3-phospho-1'-myo-inositol-3',4',5'-trisphosphate (DOPI(3,4,5)P_3), and 1-stearoyl-2-arachidonoyl- phosphatidylinositol-4',5'-bisphosphate (SAPI(4,5)P_2) were purchased from Avanti Polar Lipids. Lipids were first dissolved in water followed by dilution into 200 mM ammonium acetate containing 0.065% $C_{10}E_5$.

Native mass spectrometry (MS). Protein samples were exchanged into 200mM ammonium acetate (pH adjusted to 7.4 with ammonium hydroxide) containing 0.065% $C_{10}E_5$ using a centrifugal buffer exchange column (Micro Bio-Spin 6, Bio-Rad). The protein sample mixed with lipid was loaded into a gold-coated nanoelectrospray ionization (nESI) emitter prepared as previously described.[65] The temperature of the nESI emitter mounted on the instrument was controlled using variable temperature apparatus.[66] After the set temperature was reached the sample was incubated for several minutes before data acquisition on an Exactive Plus EMR Orbitrap Mass Spectrometer (Thermo Scientific). The instrument settings are as follows: Capillary Voltage 1.60 kV; Capillary Temperature 200 °C; Collision-Induced Dissociation (CID) 100 V; Collision Energy (CE) 10 V; Trapping gas pressure setting 3.0; Source DC offset 60V; Injection Flatpole DC 4 V; Inter Flatpole lens -20 V; Bent Flatpole DC 10 V; Transfer Multipole DC 6.

Native MS data analysis. The native MS data collected were deconvoluted using UniDec.[67] A in-house, custom software and scripts written in Python were used to assign and determine the mole fraction of apo and lipid bound states, and determining the equilibrium binding constants (discussed below). Equilibrium binding constants and thermodynamics were determined as previously described with modification.[51] In detail, the deconvoluted mass spectra text files written by UniDec from the titration series were used to determine the intensities of Kir3.2 (P) and Kir3.2-lipid (PL) species and converted to mole fraction. The apparent equilibrium association constant (K_A) for protein binding one lipid:

$$\mathrm{P} + \mathrm{L} \overset{K_A}{\leftrightarrow} \mathrm{PL}$$

$$\mathrm{K_A} = \frac{[\mathrm{PL}]}{[\mathrm{P}][\mathrm{L}]} \quad \textbf{(1)}$$

Or binding to multiple ligands:

$$\mathrm{PL}_{n-1} + \mathrm{L} \overset{\mathrm{K_A}n}{\Longleftrightarrow} \mathrm{PL}_n$$

$$\mathrm{K_A}n = \frac{[\mathrm{PL}_n]}{[\mathrm{PL}_{n-1}][\mathrm{L}]} \quad \textbf{(2)}$$

where K_{An} is the equilibrium association constant for the n_{th} ligand binding to the protein and n is the number of bound ligands. The total protein concentration ($[P]_{total}$):

$$[\mathrm{P}]_{\mathrm{total}} = [\mathrm{P}] + \sum_{i=1}^{n}[\mathrm{P}][\mathrm{L}]^i \prod_{j=1}^{i} \mathrm{K_A}j \quad \textbf{(3)}$$

Equation (2) can be rearranged to calculate the mole fraction (F_n) of PL_n:

$$\mathrm{F}_n = \frac{[\mathrm{L}]^n \prod_{j=1}^{n} \mathrm{K_A}j}{1+\sum_{i=1}^{n}[\mathrm{L}]^i \prod_{j=1}^{i} \mathrm{K_A}j} = \frac{[\mathrm{PL}_n]}{[\mathrm{P}]_{\mathrm{total}}} \quad \textbf{(4)}$$

where [L] is the free ligand concentration at equilibrium. If the concentration of protein is known, the free ligand can be calculated as follows:

$$[\mathrm{L}] = [\mathrm{L}]_{\mathrm{total}} - [\mathrm{P}]_{\mathrm{total}} \cdot \sum_{i=1}^{n} i\mathrm{F}_i \quad \textbf{(5)}$$

This sequential lipid binding model was globally fit to mole fraction data collected at a given temperature to obtain K_{An} through minimization of the pseudo-χ^2 function:[68]

$$\chi^2 = \sum_{i=0}^{n}\sum_{j=1}^{d}\left(F_{i,j,exp} - F_{i,j,calc}\right)^2 \quad \textbf{(6)}$$

where d is the number of the experimental mole fraction data points and n is the number of bound ligands.

A more complex binding model (**Figure S12**) was used in cases where the sequential lipid binding model resulted in poor fits (**Figure S11**). As Kir3.2 is known to populate two states wherein the cytoplasmic domain is in a docked and extended configuration,[55, 56] we incorporated into the binding model that lipid can bind to a fraction of Kir3.2 in either the docked or extended state. For a given lipid bound state the fractional abundance can be computed:

$$F_{PL_n} = (\propto)F_{PL_n,docked} + (1-\propto)F_{PL_n,extended} \quad \textbf{(7)}$$

where $\propto$ represents the fractional abundance of the docked state and n is the number of lipids bound. One value $\propto$ is related to an equilibrium association constant for the transition from the extended to docked state:

$$K_{ED} = \frac{\propto}{(1-\propto)} \quad \textbf{(8)}$$

Incorporating this more complex lipid binding model with one $\propto$ introduces three additional fitting parameters and divides the apo and up to two lipid bounds a fraction of two components where each component represents binding to a docked or extended state. In comparison to the

sequential binding model, the more complex lipid binding model resulted in better fits (Figure S11) and was statistically justified (F-test, $p < 0.001$). Therefore, this model was applied to determine K_{An} for each lipid-binding event. More sophisticated models were also considered, such as extending to all lipid binding events and different $\propto$s for each lipid bound state, however, they did not improve the fits and were often not statistically justified.

van't Hoff analysis[69] was used to determine the enthalpy change (ΔH), entropy change (-TΔS) and the Gibbs free energy of the binding (ΔG) based on the equation:

$$\ln K_A = -\frac{\Delta H}{R} \cdot \frac{1}{T} + \frac{\Delta S}{R} \quad \textbf{(9)}$$

Data availability

All study data are included in the article and/or SI.

Author contributions

P.Q. and A.L. designed research; P.Q., J.L., S.S., T.Z., and Y.Z. performed research; P.Q. and A.L. analyzed data; and P.Q. and A.L. wrote the paper with input from all authors.

Conflicts of interest

The are no conflicts to declare.

Acknowledgements

This work was supported by National Institutes of Health (NIH) under grant numbers DP2GM123486, R01GM121751, P41GM128577, and R01GM138863.

References

1. Touhara, K. K.; Wang, W.; MacKinnon, R., The GIRK1 subunit potentiates G protein activation of cardiac GIRK1/4 hetero-tetramers. *Elife* **2016,** *5*, e15750.
2. Lüscher, C.; Slesinger, P. A., Emerging roles for G protein-gated inwardly rectifying potassium (GIRK) channels in health and disease. *Nat Rev Neurosci* **2010,** *11* (5), 301-15.
3. Koster, J. C.; Permutt, M. A.; Nichols, C. G., Diabetes and insulin secretion: the ATP-sensitive K+ channel (K ATP) connection. *Diabetes* **2005,** *54* (11), 3065-72.
4. Ashcroft, F. M., ATP-sensitive potassium channelopathies: focus on insulin secretion. *J Clin Invest* **2005,** *115* (8), 2047-58.
5. Pattnaik, B. R.; Asuma, M. P.; Spott, R.; Pillers, D. A., Genetic defects in the hotspot of inwardly rectifying K(+) (Kir) channels and their metabolic consequences: a review. *Molecular genetics and metabolism* **2012,** *105* (1), 64-72.
6. Neusch, C.; Weishaupt, J. H.; Bahr, M., Kir channels in the CNS: emerging new roles and implications for neurological diseases. *Cell and tissue research* **2003,** *311* (2), 131-8.
7. Abraham, M. R.; Jahangir, A.; Alekseev, A. E.; Terzic, A., Channelopathies of inwardly rectifying potassium channels. *FASEB journal : official publication of the Federation of American Societies for Experimental Biology* **1999,** *13* (14), 1901-10.
8. Shieh, C. C.; Coghlan, M.; Sullivan, J. P.; Gopalakrishnan, M., Potassium channels: molecular defects, diseases, and therapeutic opportunities. *Pharmacol Rev* **2000,** *52* (4), 557-94.
9. Monica, S.-R.; Colin, G. N., Inward Rectifying Potassium Channels. In *Handbook of Ion Channels*, CRC Press: 2015; pp 241-260.
10. Hibino, H.; Inanobe, A.; Furutani, K.; Murakami, S.; Findlay, I.; Kurachi, Y., Inwardly rectifying potassium channels: their structure, function, and physiological roles. *Physiol Rev* **2010,** *90* (1), 291-366.
11. McLaughlin, S.; Murray, D., Plasma membrane phosphoinositide organization by protein electrostatics. *Nature* **2005,** *438* (7068), 605-11.
12. Huang, C. L.; Feng, S.; Hilgemann, D. W., Direct activation of inward rectifier potassium channels by PIP2 and its stabilization by Gbetagamma. *Nature* **1998,** *391* (6669), 803-6.
13. Rohacs, T.; Lopes, C. M.; Jin, T.; Ramdya, P. P.; Molnar, Z.; Logothetis, D. E., Specificity of activation by phosphoinositides determines lipid regulation of Kir channels. *Proc Natl Acad Sci U S A* **2003,** *100* (2), 745-50.
14. Fujiwara, Y.; Kubo, Y., Regulation of the desensitization and ion selectivity of ATP-gated P2X2 channels by phosphoinositides. *J Physiol* **2006,** *576* (Pt 1), 135-49.
15. Hansen, S. B.; Tao, X.; MacKinnon, R., Structural basis of PIP2 activation of the classical inward rectifier K+ channel Kir2.2. *Nature* **2011,** *477* (7365), 495-8.
16. Aryal, P.; Dvir, H.; Choe, S.; Slesinger, P. A., A discrete alcohol pocket involved in GIRK channel activation. *Nat Neurosci* **2009,** *12* (8), 988-95.
17. Ruppersberg, J. P., Intracellular regulation of inward rectifier K+ channels. *Pflugers Arch* **2000,** *441* (1), 1-11.
18. Ho, I. H.; Murrell-Lagnado, R. D., Molecular determinants for sodium-dependent activation of G protein-gated K+ channels. *J Biol Chem* **1999,** *274* (13), 8639-48.
19. Zhang, H.; He, C.; Yan, X.; Mirshahi, T.; Logothetis, D. E., Activation of inwardly rectifying K+ channels by distinct PtdIns(4,5)P2 interactions. *Nat Cell Biol* **1999,** *1* (3), 183-8.

20. Furst, O.; Mondou, B.; D'Avanzo, N., Phosphoinositide regulation of inward rectifier potassium (Kir) channels. *Front Physiol* **2014,** *4*, 404.
21. Cheng, W. W. L.; D'Avanzo, N.; Doyle, D. A.; Nichols, C. G., Dual-mode phospholipid regulation of human inward rectifying potassium channels. *Biophys J* **2011,** *100* (3), 620-628.
22. Tao, X.; Avalos, J. L.; Chen, J.; MacKinnon, R., Crystal structure of the eukaryotic strong inward-rectifier K+ channel Kir2.2 at 3.1 A resolution. *Science* **2009,** *326* (5960), 1668-74.
23. Whorton, M. R.; MacKinnon, R., Crystal structure of the mammalian GIRK2 K+ channel and gating regulation by G proteins, PIP2, and sodium. *Cell* **2011,** *147* (1), 199-208.
24. Whorton, M. R.; MacKinnon, R., X-ray structure of the mammalian GIRK2-betagamma G-protein complex. *Nature* **2013,** *498* (7453), 190-7.
25. Lopes, C. M.; Zhang, H.; Rohacs, T.; Jin, T.; Yang, J.; Logothetis, D. E., Alterations in conserved Kir channel-PIP2 interactions underlie channelopathies. *Neuron* **2002,** *34* (6), 933-44.
26. Zangerl-Plessl, E. M.; Qile, M.; Bloothooft, M.; Stary-Weinzinger, A.; van der Heyden, M. A. G., Disease Associated Mutations in K(IR) Proteins Linked to Aberrant Inward Rectifier Channel Trafficking. *Biomolecules* **2019,** *9* (11).
27. Hedger, G.; Sansom, M. S. P., Lipid interaction sites on channels, transporters and receptors: Recent insights from molecular dynamics simulations. *Biochim Biophys Acta* **2016,** *1858* (10), 2390-2400.
28. Corey, R. A.; Vickery, O. N.; Sansom, M. S. P.; Stansfeld, P. J., Insights into Membrane Protein–Lipid Interactions from Free Energy Calculations. *Journal of Chemical Theory and Computation* **2019,** *15* (10), 5727-5736.
29. Pipatpolkai, T.; Corey, R. A.; Proks, P.; Ashcroft, F. M.; Stansfeld, P. J., Evaluating inositol phospholipid interactions with inward rectifier potassium channels and characterising their role in disease. *Communications Chemistry* **2020,** *3* (1), 147.
30. Corradi, V.; Mendez-Villuendas, E.; Ingolfsson, H. I.; Gu, R. X.; Siuda, I.; Melo, M. N.; Moussatova, A.; DeGagne, L. J.; Sejdiu, B. I.; Singh, G.; Wassenaar, T. A.; Delgado Magnero, K.; Marrink, S. J.; Tieleman, D. P., Lipid-Protein Interactions Are Unique Fingerprints for Membrane Proteins. *ACS Cent Sci* **2018,** *4* (6), 709-717.
31. Rohacs, T.; Chen, J.; Prestwich, G. D.; Logothetis, D. E., Distinct specificities of inwardly rectifying K(+) channels for phosphoinositides. *J Biol Chem* **1999,** *274* (51), 36065-72.
32. D'Avanzo, N.; Cheng, W. W.; Doyle, D. A.; Nichols, C. G., Direct and specific activation of human inward rectifier K+ channels by membrane phosphatidylinositol 4,5-bisphosphate. *J Biol Chem* **2010,** *285* (48), 37129-32.
33. D'Avanzo, N.; Lee, S.-J.; Cheng, W. W. L.; Nichols, C. G., Energetics and location of phosphoinositide binding in human Kir2.1 channels. *The Journal of biological chemistry* **2013,** *288* (23), 16726-16737.
34. Wang, W.; Whorton, M. R.; MacKinnon, R., Quantitative analysis of mammalian GIRK2 channel regulation by G proteins, the signaling lipid PIP2 and Na+ in a reconstituted system. *Elife* **2014,** *3*, e03671-e03671.
35. Qiao, P.; Liu, Y.; Zhang, T.; Benavides, A.; Laganowsky, A., Insight into the selectivity of Kir3.2 toward phosphatidylinositides. *Biochemistry* **2020**.
36. Agasid, M. T.; Robinson, C. V., Probing membrane protein-lipid interactions. *Curr Opin Struct Biol* **2021,** *69*, 78-85.

37. Laganowsky, A.; Reading, E.; Allison, T. M.; Ulmschneider, M. B.; Degiacomi, M. T.; Baldwin, A. J.; Robinson, C. V., Membrane proteins bind lipids selectively to modulate their structure and function. *Nature* **2014,** *510* (7503), 172-5.
38. Allison, T. M.; Reading, E.; Liko, I.; Baldwin, A. J.; Laganowsky, A.; Robinson, C. V., Quantifying the stabilizing effects of protein-ligand interactions in the gas phase. *Nat Commun* **2015**, in press.
39. Fantin, S. M.; Parson, K. F.; Niu, S.; Liu, J.; Polasky, D. A.; Dixit, S. M.; Ferguson-Miller, S. M.; Ruotolo, B. T., Collision Induced Unfolding Classifies Ligands Bound to the Integral Membrane Translocator Protein. *Anal Chem* **2019,** *91* (24), 15469-15476.
40. Cong, X.; Liu, Y.; Liu, W.; Liang, X.; Laganowsky, A., Allosteric modulation of protein-protein interactions by individual lipid binding events. *Nat Commun* **2017,** *8* (1), 2203.
41. Yen, H. Y.; Hoi, K. K.; Liko, I.; Hedger, G.; Horrell, M. R.; Song, W.; Wu, D.; Heine, P.; Warne, T.; Lee, Y.; Carpenter, B.; Pluckthun, A.; Tate, C. G.; Sansom, M. S. P.; Robinson, C. V., PtdIns(4,5)P2 stabilizes active states of GPCRs and enhances selectivity of G-protein coupling. *Nature* **2018,** *559* (7714), 423-427.
42. Patrick, J. W.; Boone, C. D.; Liu, W.; Conover, G. M.; Liu, Y.; Cong, X.; Laganowsky, A., Allostery revealed within lipid binding events to membrane proteins. *Proc Natl Acad Sci U S A* **2018,** *115* (12), 2976-2981.
43. Barrera, N. P.; Di Bartolo, N.; Booth, P. J.; Robinson, C. V., Micelles protect membrane complexes from solution to vacuum. *Science* **2008,** *321* (5886), 243-6.
44. Gault, J.; Donlan, J. A.; Liko, I.; Hopper, J. T.; Gupta, K.; Housden, N. G.; Struwe, W. B.; Marty, M. T.; Mize, T.; Bechara, C.; Zhu, Y.; Wu, B.; Kleanthous, C.; Belov, M.; Damoc, E.; Makarov, A.; Robinson, C. V., High-resolution mass spectrometry of small molecules bound to membrane proteins. *Nat Methods* **2016,** *13* (4), 333-6.
45. Marcoux, J.; Wang, S. C.; Politis, A.; Reading, E.; Ma, J.; Biggin, P. C.; Zhou, M.; Tao, H.; Zhang, Q.; Chang, G.; Morgner, N.; Robinson, C. V., Mass spectrometry reveals synergistic effects of nucleotides, lipids, and drugs binding to a multidrug resistance efflux pump. *Proc Natl Acad Sci U S A* **2013,** *110* (24), 9704-9.
46. Yen, H. Y.; Hopper, J. T. S.; Liko, I.; Allison, T. M.; Zhu, Y.; Wang, D.; Stegmann, M.; Mohammed, S.; Wu, B.; Robinson, C. V., Ligand binding to a G protein-coupled receptor captured in a mass spectrometer. *Sci Adv* **2017,** *3* (6), e1701016.
47. Bolla, J. R.; Sauer, J. B.; Wu, D.; Mehmood, S.; Allison, T. M.; Robinson, C. V., Direct observation of the influence of cardiolipin and antibiotics on lipid II binding to MurJ. *Nat Chem* **2018,** *10* (3), 363-371.
48. Marcoux, J.; Robinson, C. V., Twenty years of gas phase structural biology. *Structure* **2013,** *21* (9), 1541-50.
49. Liu, Y.; LoCaste, C. E.; Liu, W.; Poltash, M. L.; Russell, D. H.; Laganowsky, A., Selective binding of a toxin and phosphatidylinositides to a mammalian potassium channel. *Nat Commun* **2019,** *10* (1), 1352.
50. van't Hoff, M. J. H., Etudes de dynamique chimique. *Recueil des Travaux Chimiques des Pays-Bas* **1884,** *3* (10), 333-336.
51. Cong, X.; Liu, Y.; Liu, W.; Liang, X.; Russell, D. H.; Laganowsky, A., Determining Membrane Protein-Lipid Binding Thermodynamics Using Native Mass Spectrometry. *J Am Chem Soc* **2016,** *138* (13), 4346-9.

52. Reading, E.; Liko, I.; Allison, T. M.; Benesch, J. L.; Laganowsky, A.; Robinson, C. V., The role of the detergent micelle in preserving the structure of membrane proteins in the gas phase. *Angew Chem Int Ed Engl* **2015,** *54* (15), 4577-81.
53. McCabe, J. W.; Shirzadeh, M.; Walker, T. E.; Lin, C. W.; Jones, B. J.; Wysocki, V. H.; Barondeau, D. P.; Clemmer, D. E.; Laganowsky, A.; Russell, D. H., Variable-Temperature Electrospray Ionization for Temperature-Dependent Folding/Refolding Reactions of Proteins and Ligand Binding. *Anal Chem* **2021,** *93* (18), 6924-6931.
54. Marty, M. T.; Baldwin, A. J.; Marklund, E. G.; Hochberg, G. K.; Benesch, J. L.; Robinson, C. V., Bayesian deconvolution of mass and ion mobility spectra: from binary interactions to polydisperse ensembles. *Anal Chem* **2015,** *87* (8), 4370-6.
55. Niu, Y.; Tao, X.; Touhara, K. K.; MacKinnon, R., Cryo-EM analysis of PIP2 regulation in mammalian GIRK channels. *eLife* **2020,** *9*, e60552.
56. Mathiharan, Y. K.; Glaaser, I. W.; Zhao, Y.; Robertson, M. J.; Skiniotis, G.; Slesinger, P. A., Structural insights into GIRK2 channel modulation by cholesterol and PIP2. *Cell Reports* **2021,** *36* (8), 109619.
57. Dill, K. A., Dominant forces in protein folding. *Biochemistry* **1990,** *29* (31), 7133-55.
58. Dragan, A. I.; Read, C. M.; Crane-Robinson, C., Enthalpy-entropy compensation: the role of solvation. *Eur Biophys J* **2017,** *46* (4), 301-308.
59. Frederick, K. K.; Marlow, M. S.; Valentine, K. G.; Wand, A. J., Conformational entropy in molecular recognition by proteins. *Nature* **2007,** *448* (7151), 325-9.
60. Tzeng, S. R.; Kalodimos, C. G., Dynamic activation of an allosteric regulatory protein. *Nature* **2009,** *462* (7271), 368-72.
61. Tzeng, S. R.; Kalodimos, C. G., Protein activity regulation by conformational entropy. *Nature* **2012,** *488* (7410), 236-40.
62. Caro, J. A.; Harpole, K. W.; Kasinath, V.; Lim, J.; Granja, J.; Valentine, K. G.; Sharp, K. A.; Wand, A. J., Entropy in molecular recognition by proteins. *Proc Natl Acad Sci U S A* **2017,** *114* (25), 6563-6568.
63. O'Brien, E. S.; Fuglestad, B.; Lessen, H. J.; Stetz, M. A.; Lin, D. W.; Marques, B. S.; Gupta, K.; Fleming, K. G.; Wand, A. J., Membrane Proteins Have Distinct Fast Internal Motion and Residual Conformational Entropy. *Angewandte Chemie International Edition* **2020,** *59* (27), 11108-11114.
64. Scholz, J.; Suppmann, S., A new single-step protocol for rapid baculovirus-driven protein production in insect cells. *BMC Biotechnol* **2017,** *17* (1), 83.
65. Laganowsky, A.; Reading, E.; Hopper, J. T. S.; Robinson, C. V., Mass spectrometry of intact membrane protein complexes. *Nature Protocols* **2013,** *8* (4), 639-651.
66. McCabe, J. W.; Shirzadeh, M.; Walker, T. E.; Lin, C.-W.; Jones, B. J.; Wysocki, V. H.; Barondeau, D. P.; Clemmer, D. E.; Laganowsky, A.; Russell, D. H., Variable-Temperature Electrospray Ionization for Temperature-Dependent Folding/Refolding Reactions of Proteins and Ligand Binding. *Analytical Chemistry* **2021,** *93* (18), 6924-6931.
67. Marty, M.; Baldwin, A.; Marklund, E.; Hochberg, G.; Benesch, J.; Robinson, C. V., Bayesian Deconvolution of Mass and Ion Mobility Spectra: From Binary Interactions to Polydisperse Ensembles. *Anal. Chem.* **2015,** *87*, 4370-4376.

68. Stengel, F.; Baldwin, A. J.; Bush, M. F.; Hilton, G. R.; Lioe, H.; Basha, E.; Jaya, N.; Vierling, E.; Benesch, J. L., Dissecting heterogeneous molecular chaperone complexes using a mass spectrum deconvolution approach. *Chem Biol* **2012,** *19* (5), 599-607.
69. van't Hoff, M. J. H., Etudes de dynamique chimique. *Recl. Trav. Chim. Pays-Bas* **1884,** *3* (10), 333-336.

Figures

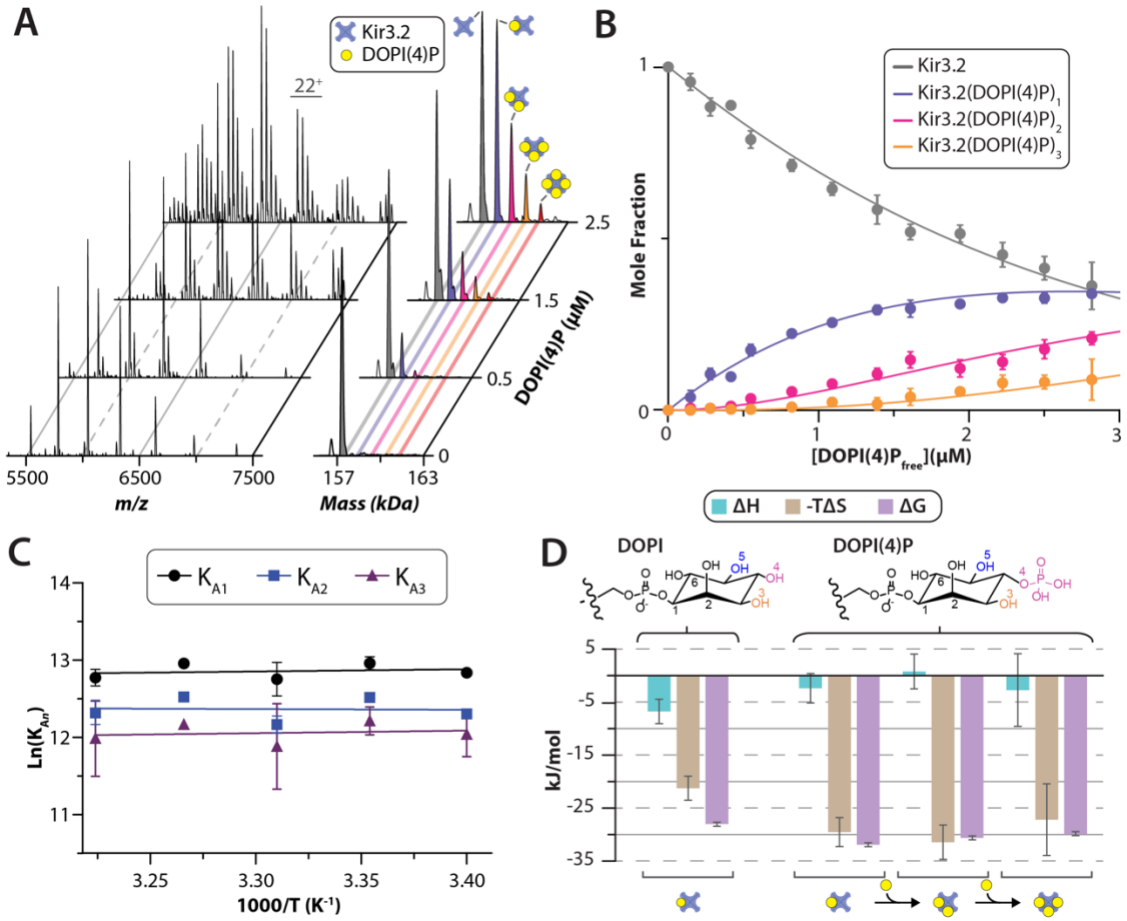

Figure 1. Determination of binding thermodynamics for Kir3.2-lipid interactions. A) Representative native mass spectra and their deconvolution from a titration series of Kir3.2 with dioleoyl (18:1-18:1) phosphatidylinositol 4-phosphate (DOPI(4)P) recorded at 298 K. Kir3.2 and the various lipid bound states of Kir3.2 are labeled. B) Plot of the mole fraction for Kir3.2 and Kir3.2•DOPI(4)P_{1-3} bound states of Kir3.2 determined from a titration series and resulting fit (R^2 = 0.99) of a sequential lipid binding model (lines). C) van't Hoff plot for Kir3.2 binding Kir3.2•DOPI(4)P_{1-3} (dots) and regression of linear equations (solid lines) to deduce thermodynamics for each lipid binding event. D) Thermodynamics of dioleoyl DOPI(4)P and phosphatidylinositol (DOPI) binding Kir3.2 at 298 K. The first, second, and third lipid (labeled as 1x–3x) is shown for DOPI(4)P. Shown above are the headgroup structures with the 3', 4', and 5' positions of the inositol headgroup colored orange, pink, and blue, respectively. Reported are the average and s.e.m. from repeated measurements (n = 3).

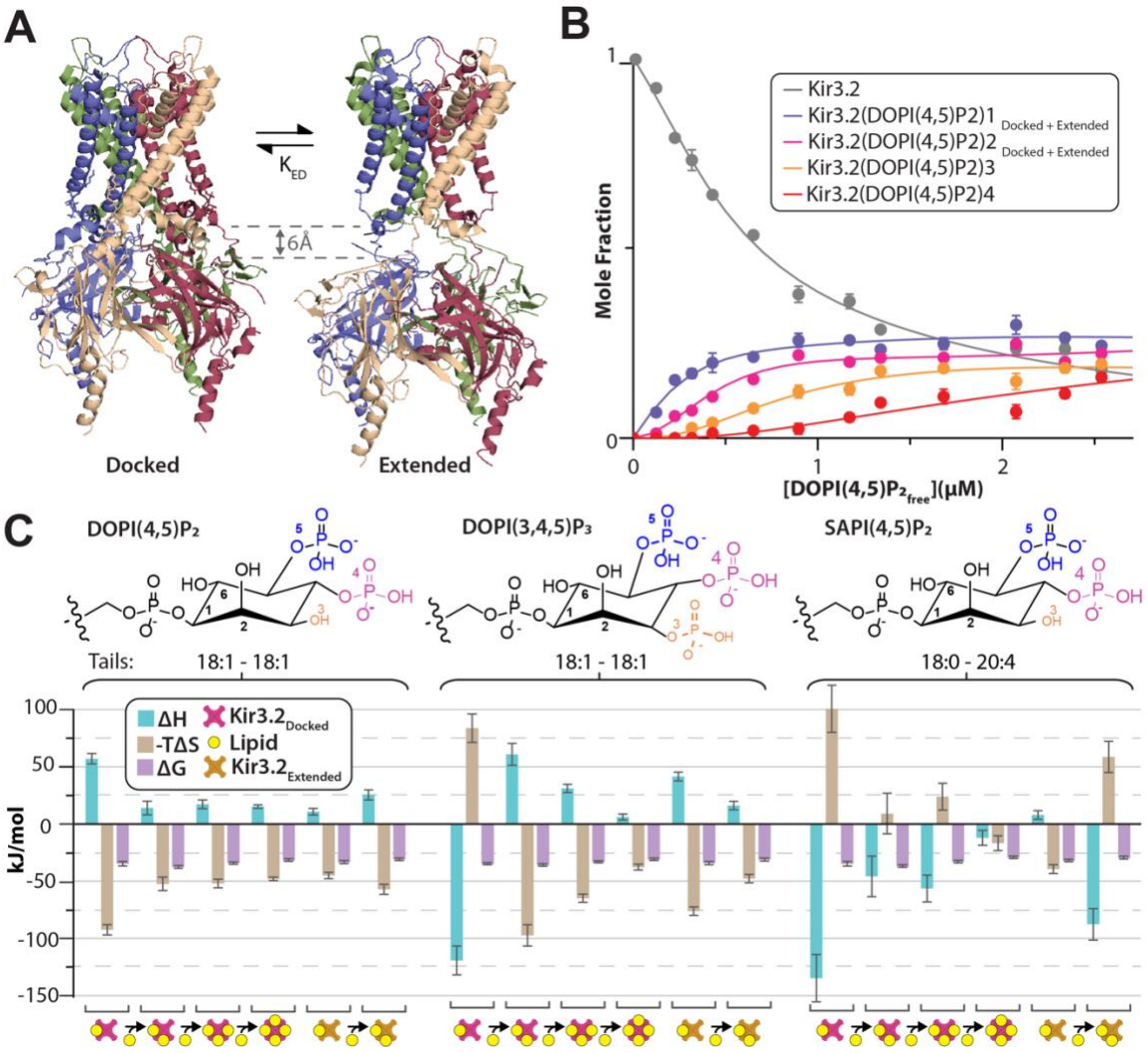

Figure 2. Thermodynamic signatures of specific phosphoinositides binding to different states of Kir3.2. A) Structures of Kir2.2 in the docked (PDB 3SPI) and extended states (PDB 3JYC) shown in cartoon representation. The phosphatidylinositol 4,5-bisphosphate (PI(4,5)P_2) with 8:0-8:0 tails bound to the docked state is also shown. B) Plot of the mole fraction of Kir3.2 and the channel bound to PI(4,5)P_2 with DO tails (DOPI(4,5)P_2). Resulting fit (solid lines, R^2 = 0.99) of lipid binding model where the lipid can bind to either the docked or extended states of Kir3.2. C) Binding thermodynamics for DOPI(4,5)P_2, phosphatidylinositol 3,4,5-trisphosphate with DO tails (DOPI(3,4,5)P_3), and PI(4,5)P_2 with 1-stearoyl-2-arachidonoyl (18:0-20:4) tails (SAPI(4,5)P_2) to Kir3.2 determined through van't Hoff analysis for binding to the docked and extended states at 298 K. Reported are the average and s.e.m. from repeated measurements (n = 3).

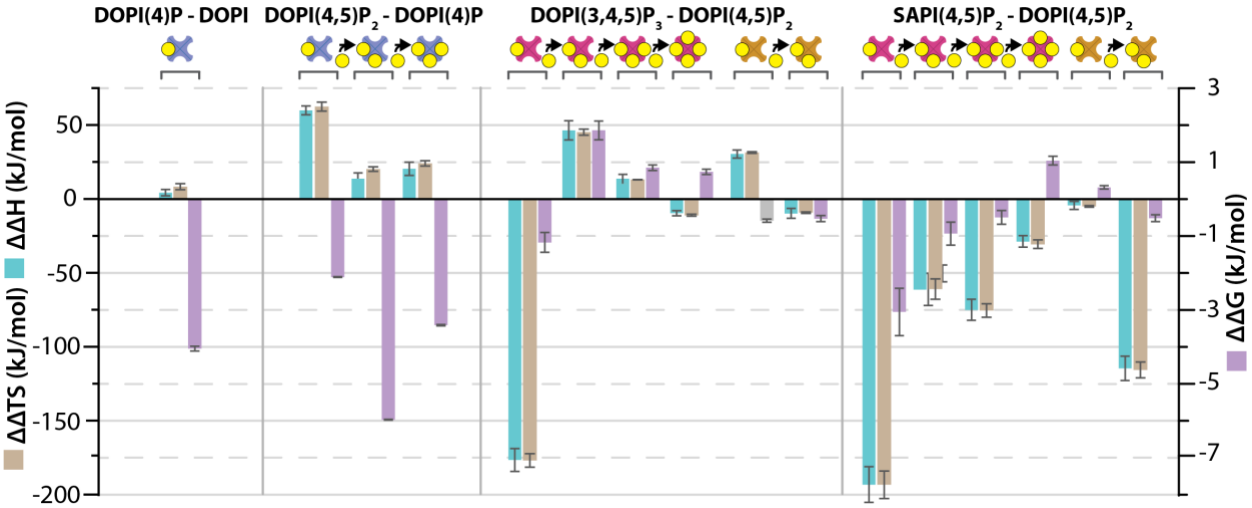

Figure 3. Alterations in thermodynamic signatures for the stepwise transition from DOPI to DOPI(3,4,5)P_3 and acyl chain chemistry of PI(4,5)P_2. Values were computed using a temperature of 298K. Shown as described in Figure 2. Reported are the average and s.e.m. (n=3).